AFRL-RV-PS-
TR-2012-0127

# ADVANCED SPACE-BASED DETECTORS

**David Cardimona and Dan Hanhuang**

**24 Sep 2012**

**Interim Report**




**AIR FORCE RESEARCH LABORATORY**
**Space Vehicles Directorate**
**3550 Aberdeen Ave SE**
**AIR FORCE MATERIEL COMMAND**
**KIRTLAND AIR FORCE BASE, NM 87117-5776**

# DTIC COPY
# NOTICE AND SIGNATURE PAGE



AFRL-RV-PS-TR-2012-0127 HAS BEEN REVIEWED AND IS APPROVED FOR PUBLICATION IN ACCORDANCE WITH ASSIGNED DISTRIBUTION STATEMENT

//signed//
DAVID CARDIMONA
Program Manager

//signed//
PAUL D. LEVAN, Ph.D.
Technical Advisor, Space Based Advanced Sensing and Protection

//signed//
B. SINGARAJU, Ph.D.
Deputy Chief, Spacecraft Technology Division
Space Vehicles Directorate

# REPORT DOCUMENTATION PAGE

*Form Approved*
*OMB No. 0704-0188*



| 1. REPORT DATE *(DD-MM-YY)* | 2. REPORT TYPE | 3. DATES COVERED *(From - To)* |
|---|---|---|
| 24-09-2012 | Interim Report | 8 Jan 2010 – 29 Jan 2012 |

**4. TITLE AND SUBTITLE**

Advanced Space-Based Detectors

**5a. CONTRACT NUMBER**

**5b. GRANT NUMBER**

**5c. PROGRAM ELEMENT NUMBER**
62601F

**6. AUTHOR(S)**

David Cardimona and Dan Hanhaung

**5d. PROJECT NUMBER**
4846

**5e. TASK NUMBER**
PPM00004410

**5f. WORK UNIT NUMBER**
EF002011

**7. PERFORMING ORGANIZATION NAME(S) AND ADDRESS(ES)**

Air Force Research Laboratory
Space Vehicles Directorate
3550 Aberdeen Ave., SE
Kirtland AFB, NM 87117-5776

**8. PERFORMING ORGANIZATION REPORT NUMBER**

AFRL-RV-PS-TR-2012-0127

**9. SPONSORING / MONITORING AGENCY NAME(S) AND ADDRESS(ES)**

**10. SPONSOR/MONITOR'S ACRONYM(S)**
AFRL/RVSS

**11. SPONSOR/MONITOR'S REPORT NUMBER(S)**

**12. DISTRIBUTION / AVAILABILITY STATEMENT**

Approved for public release; Distribution Unlimited. (377ABW-2011-1560 dtd 7 Nov 2011)

**13. SUPPLEMENTARY NOTES**

**14. ABSTRACT**

For this in-house project, we are interested in improving the performance or modifying the capabilities of infrared detectors in order to locate and identify dim and/or distant objects in space. One characteristic we are very interested in is multicolor detection. To this end, we have turned to a novel detector design that we have come to call a Lateral Quantum Dot Infrared Photodetector (LQDIP). In this design, InAs quantum dots are buried in a GaAs quantum well, which in turn is tunnel-coupled to another GaAs quantum well. Photoexcited electrons from the quantum dots tunnel over to the second well and are then swept out via a lateral (perpendicular to the growth direction) bias voltage. This architecture should exhibit the ability to tune to select infrared frequencies with reduced dark current and unity gain. The lateral photocurrent is directed by a vertical (parallel to the growth direction) gate voltage. In this interim report, we will discuss this detector architecture, as well as our preliminary electrical and optical characterization results from 200K to 77K.

**15. SUBJECT TERMS**

Infrared, Detectors, Quantum Well Detectors, Superlattice Detectors, Quantum Dot Detectors

| 16. SECURITY CLASSIFICATION OF: | | | 17. LIMITATION OF ABSTRACT | 18. NUMBER OF PAGES | 19a. NAME OF RESPONSIBLE PERSON |
|---|---|---|---|---|---|
| a. REPORT | b. ABSTRACT | c. THIS PAGE | | | 19b. TELEPHONE NUMBER *(include area code)* |
| Unclassified | Unclassified | Unclassified | Unlimited | 22 | David Cardimona |

(This page intentionally left blank)

# 1 INTRODUCTION

## 1.1 Motivation

The Air Force Research Laboratory Space Vehicles Directorate has a need to provide the US Air Force with space based infrared (IR) detectors, capable of producing timely, accurate, multi-color detection of space and ground based objects via day and night remote sensing. These objects of interest may be in Low Earth Orbit, Medium Earth Orbit, or Geosynchronous Orbit, have background levels as low as $10^9$ photons/cm$^2$/s, and be at ranges greater than 100 km away from the sensing platform. Space-based detectors must also be radiation hardened to survive the high levels of protons, electrons and cosmic rays present in the space environment. Current infrared focal plane arrays (FPAs) are mostly capable of fulfilling all these requirements, but are extremely costly to design and manufacture, especially for multi-color detection. Most importantly, to achieve any level of multi-color detection these FPAs must usually be operated with spectral filters, each with complementary optics.[1-2] It would be ideal to be able to achieve multi-color sensing with a single FPA via an internally voltage-tunable, narrowband spectral response. This would remove the need for multiple FPAs and spectral filters, as well as all of their supporting equipment, thereby reducing the satellite launch payload weight and cost.

The detector described herein, henceforth referred to as a Lateral Quantum Dot Infrared Photodetector (LQDIP), is expected to have an internally continuously voltage-tunable, narrowband spectral response, something not directly achievable with current bulk-style IR detectors. This interim report will discuss the LQDIP detector architecture, operating principles and conditions, and preliminary results of I-V, photocurrent and differential conductance measurements.

### 1.2 LQDIP Growth Structure and Device Layout

The LQDIP material structure and device layout are both depicted in Fig. 1. The detector material was grown by Molecular Beam Epitaxy (MBE) on a GaAs semi-insulating substrate. As Fig. 1a shows, the material structure is an asymmetric double quantum well that is grown as follows. First, a 200 nm GaAs buffer layer is grown on top of the substrate material. This is followed by a 60 nm $Al_{0.3}Ga_{0.7}As$ bottom barrier and then a 7.5 nm, undoped GaAs bottom quantum well, the so-called *tuning* well. A narrow 5 nm $Al_{0.3}Ga_{0.7}As$ middle barrier layer is grown next, followed by a 4 nm GaAs top quantum well, which is embedded with n-doped, InAs quantum dots. The latter is the so-called *dots-in-a-well (DWELL) absorbing layer*. The quantum dots in this DWELL layer are grown via the Stranski–Krastanov growth mode. The doping-level-to-dot-density ratio is expected to result in roughly 3 electrons per dot, which equates to a doping level of ~ 6.35 x $10^{18}$ $cm^{-3}$. Following the DWELL absorbing layer a 60 nm $Al_{0.3}Ga_{0.7}As$ top barrier layer is grown to complete the wafer stack. Preliminary Schrodinger-Poisson calculations for this wafer stack predict two quantum well states centered in the tuning well layer at ~ 35 meV and ~ 135 meV above the GaAs conduction band edge; multiple quantum dot energy levels are expected to arise in the DWELL layer starting at roughly -121 meV below it.[3] Using this material, samples similar to the device layout in Fig. 1b were fabricated. A 100 x 500 μm rectangular mesa was etched and ohmic source and drain contacts were formed on two opposing sidewalls of the mesa. Following this, a narrow, Ti-Au pinch-off gate was deposited directly on top of the mesa, close to one of the ohmic contacts on the side of the mesa. To test the design at cryogenic temperatures, one sample was mounted and wirebonded to a 68-pin Leadless Chip Carrier (LCC) that fits within a cryogenic dewar.

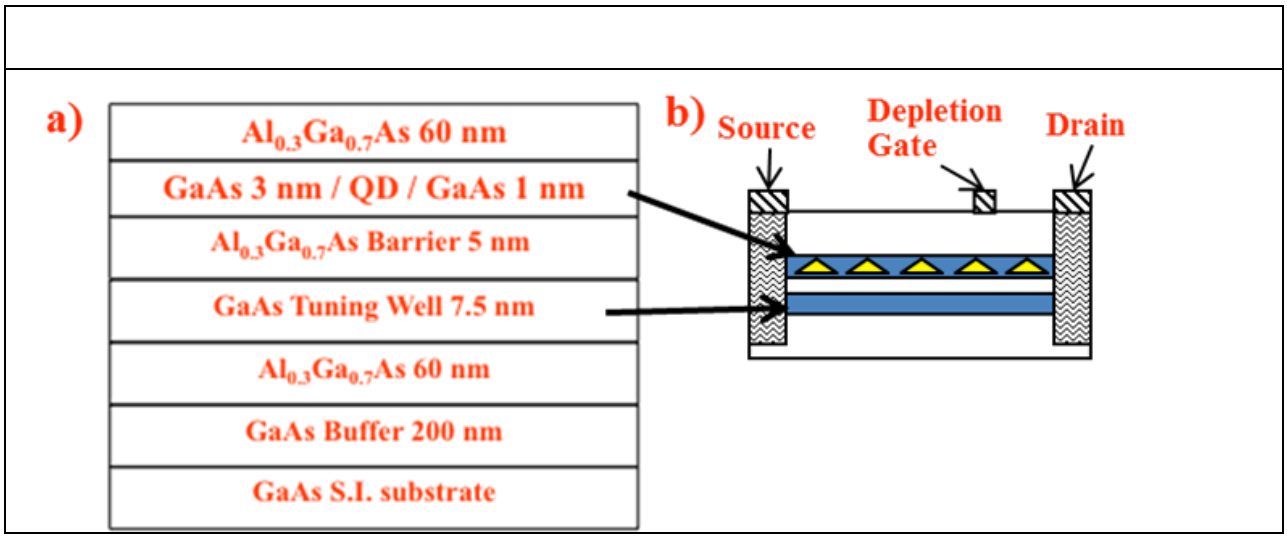


Figure 1. Cartoon schematic depicting the (a) growth structure and (b) device layout of the LQDIP. Differently hatched areas on the device layout schematic reflect the ohmics source and drain contacts and the depletion gate

### 1.3 LQDIP Operation and Bias Conditions

The LQDIP detector structure ideally functions as follows. With the proper source-drain and pinch-off gate biasing discussed further below, the top quantum well, the DWELL-layer containing the self-assembled InAs quantum dots, acts as the infrared absorber, while the undoped bottom quantum well layer, the tuning well, serves as a unity-gain transport channel. As the source-drain ohmic contacts in the LQDIP are on opposite sidewalls of the mesa, the current at low temperatures is expected to flow laterally in the plane of each quantum well; this is in direct contrast with most photodetectors, such as typical quantum dot infrared photodetectors (QDIPs), where the current flows vertically between the ohmic contacts on the mesa top and bottom. The doping in the DWELL absorbing layer will allow for some conduction in that well, albeit in the presence of multiple sources of scattering including ionized impurities and with the possibility of recapture by the quantum dots. The expected presence of ionized impurity scattering and the consequent reduction in the DWELL layer conduction is not necessarily detrimental, however, since ultimately conduction across the entire absorbing DWELL layer is not desirable for LQDIP operation. As discussed further below, conduction in that layer is ideally

deliberately blocked by the presence of a depletion-field-induced barrier from a narrow pinch-off gate on top of the mesa device and photocarriers generated in that layer are expected to vertically tunnel through the AlGaAs barrier to the tuning well below to be read out.

Much lower, to near zero, conduction is initially expected in the undoped tuning well compared with the DWELL layer as carriers originating in the latter must be made to enter the tuning well either by photo- or thermal-excitation. Once these carriers arrive in the tuning well, however, they are expected to undergo minimal scattering and have zero recapture probability as they flow laterally across the mesa to the drain contact. The possibility for recapture of photo-excited carriers by quantum dots is the same mechanism that leads to less than unity gain in vertical QDIPs, where photoconductive gain is inversely proportional to recapture probability. The recapture mechanism is not expected to occur in the LQDIP, however, once the photo-excited carriers have tunneled into the tuning well. This lack of recapture in the tuning well would thus equate to a near unity gain as every photo-excited carrier that tunnels into it is expected be read out.

Under illumination, photons preferentially excite carriers in the dots to a virtual excited state in the DWELL, expected to form by the strong coupling to the ground state of the nearby tuning well. Photon-assisted tunneling, via this virtual state, allows the photoexcited carriers to tunnel into the tuning layer, where they again quickly traverse to the drain contact. Tuning of the spectral response is ideally achieved by changing the lateral source-drain bias, which under proper pinch-off gate biasing, discussed below, transforms into an effective vertical bias that falls mainly across the barrier between the two wells. This vertical bias adjusts the relative vertical alignment between the energy levels in each well, as depicted in Fig. 2, leading to a change in the detector spectral response.[4]

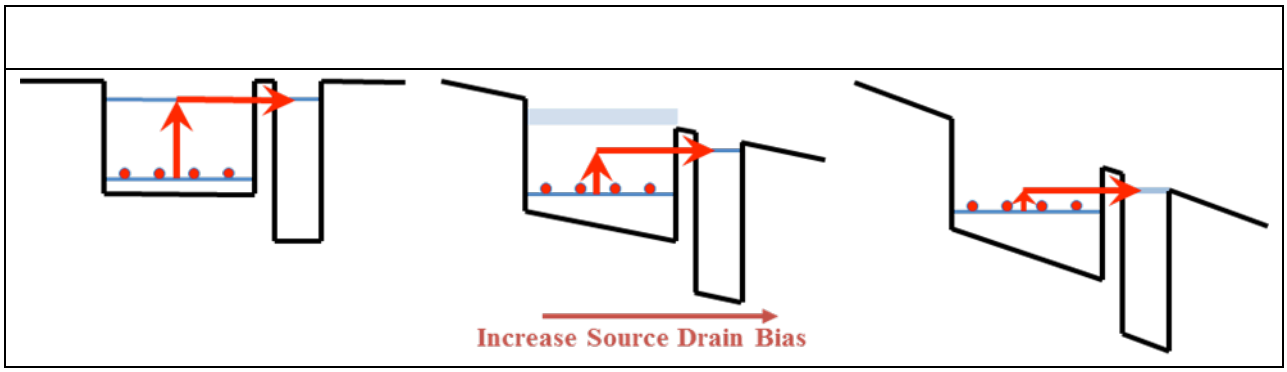


Figure 2: Cartoon schematic of the potentially, continuous tuning, photon-assisted tunneling scheme. The schematic depicts the change in the detector's spectral response to longer wavelengths as the source drain bias increases.

Determining the proper pinch-off gate bias operating conditions requires measuring the source-drain current as a function of pinch-off gate voltage. As Fig. 3 depicts, the lateral current in the LQDIP can be blocked by applying a negative bias voltage to the pinch-off gate. The negative pinch-off gate voltage produces an electric field that depletes the electron density in the region directly beneath the pinch-off gate, leading to an increase in the resistance of the affected layers and consequent reduction in the measured current. This field-effect behavior is exactly similar to that of a depletion-mode MOSFET. Lateral current should continue decreasing as the gate voltage is made more negative, first completely pinching off the current flow in the DWELL layer and then, eventually, eliminating any conduction in the tuning well below it.

The expected operating scheme is thus to have the pinch-off gate voltage adjusted such that conduction in the DWELL, the top quantum well, is completely pinched off while conduction in the tuning well is not affected, which is the scenario depicted in the middle cartoon schematic of Fig. 3. Here, the source-drain bias gets transformed into a vertical bias, as was discussed above, across the middle $Al_{0.3}Ga_{0.7}As$ barrier between the two wells and the only source-drain current that ideally remains will be due to any electrons in the absorbing layer that can resonantly tunnel into the tuning well. For low temperature operation, these electrons are predominantly the photo-

excited carriers created by the incoming photons with energy exactly equal to the difference between the quantum dot ground state and the virtual excited state energies. Thus, by altering the source-drain bias this energy difference can be changed and consequently frequency agile detection becomes possible. Finally, any leakage current from the pinch-off gate to the drain contact needs to be much smaller than the source-drain current.

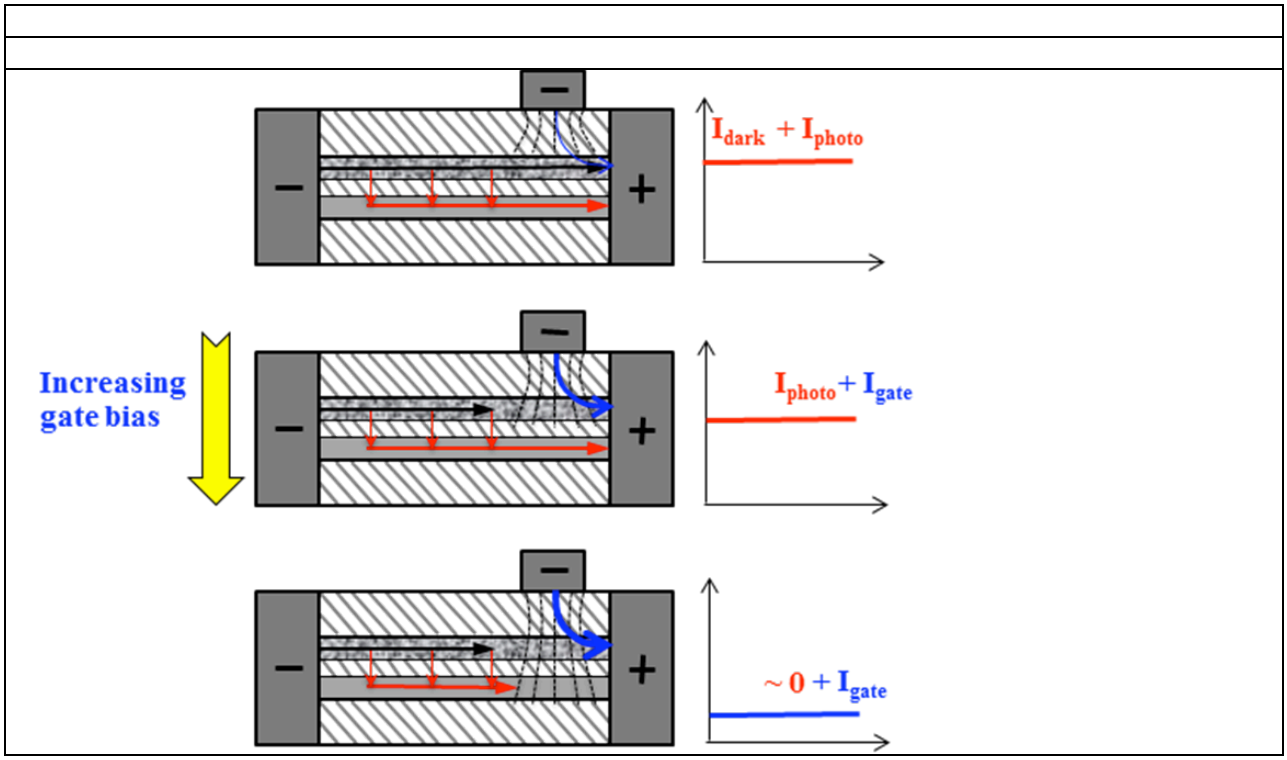


Figure 3: Cartoon schematic showing the ideal effect that increasing the gate bias has on the measured signal.

Beyond the potential ability to tune the detector's spectral response, the LQDIP architecture should ideally inherit some of the other benefits native to DWELL, QDIP, and QWIP detectors. These benefits may include: a low source to drain bias voltage, response to normally incident light, high operating temperature, and low dark current.[6-11] High in-plane mobility, due to the quantum well, should allow the detector to operate at high speed with a very low source-drain bias voltage. The use of a DWELL layer as an absorber allows for the detection of normally incident light and a low dark current due to a decrease in the thermionic emission of carrier.

# 2. EXPERIMENTAL SETUP

## 2.1 I-V Test Bed

The LQDIP was mounted and wirebonded to a 68 pin LCC for testing. The LCC was fastened to the cold-finger of a pour-filled cryogenic dewar capable of reaching 4 K. The dewar was pumped down to a vacuum of $5x10^{-7}$ Torr and cryogenically cooled to 77 K with liquid nitrogen. The dark current measurements were taken with a cold shield surrounding the device, which was also cooled to 77 K, blocking nearly all infrared radiation. Two Keithley Model 236 Source Measurement Units were used to apply the source-drain and gate voltages. A Lakeshore Model 340 Temperature Controller monitored the temperature of the detector via a diode fastened to the cold finger. Source-drain voltages from -1.0 V to 1.0 V were applied across the device while simultaneous current measurements were made. The gate voltages ranged from 0.0 V to -0.8 V.

## 2.2 Differential Conductance Test Bed

A similar sample mounting scheme was used for taking differential conductance measurements. Here, a small 13 Hz, 100 μV AC signal, output from a Stanford Research Systems Model SR850 DSP Lock-In Amplifier, was passed to an external, ambient temperature, 10 MΩ resistor connected in series to the drain contact of the LQDIP, with its source contact grounded. This setup allows the differential conductance of the LQDIP to be measured via low frequency lock-in measurements of the voltage across the 10 MΩ resistor. Measurements of the differential conductance were also taken as the gate voltage was swept from 0.0 V to -0.85 V.

## 2.3 Optical Measurements

Simple DC photocurrent measurements were also taken with a cold shield, cooled to 77 K, in place and having a hole cut in one side to allow for incident 300 K blackbody radiation. The radiation passed into the dewar through a KRS5 window, leading to ~ f/2 optical alignment.

These photocurrent measurements demonstrate the LQDIP has an optical response and functions as an infrared detector. Furthermore, they allowed for the gating properties to be measured in the presence of illumination.

With only a single layer of quantum dots present in the absorbing layer, the absorption properties of this LQDIP are understandably weak. Coupled with the relatively small size of the particular LQDIP under investigation, this precluded spectral response measurements from being performed in the available spectral response measurement system, a Nicolet Magna 860 FTIR, and thus a full performance characterization has not yet been accomplished. The FTIR spectral response setup is currently being upgraded to allow for step-scan/lock-in style measurements, which would allow very sensitive spectral response measurements to be performed on this particular detector. Normal vertical QDIPs, in contrast to this LQDIP, typically have 10-15 layers of quantum dots to increase the amount of absorption that occurs in them. A scheme to allow for multiple DWELL layers in future variants of the LQDIP has been envisioned using regrowth techniques and is currently being pursued by a collaborator.[12]

## 3. RESULTS AND DISCUSSION

### 3.1 I-V Characterization Results

The dark current in the LQDIP was measured at 77 K with the DC source-drain voltage being stepped in 1.0 mV increments from - 1.0 V to 1.0 V. The absolute value of the measured source-drain current $I_{SD}$ was plotted with respect to the varied source-drain voltage $V_{SD}$. This measurement was repeated at different gate voltages $V_{Gate}$ of 0.1 V increments, from 0.0 V to -0.8 V. The results are plotted in Fig. 4. They show the dark current in the 0.0 V to 1.0 V region reduces as the gate voltage becomes more negative, which is consistent with the behavior of a properly functioning depletion gate as described in section 1.3. At the largest gate voltage $V_{gate}$ =

- 0.8 V, the source-drain current is on the order of 50 pA. Thus, if current was confined solely to the quantum wells, which have a relevant area of 100 µm x 11.5 nm, the width of the mesa and width of both quantum wells, respectively, the dark current density is ~ 4.3 mA/cm$^2$. Applying a different perspective, however, this 50 pA dark current is also for a device with an optical area on the order of 100 µm x 500 µm; using that as the relevant area leads to a dark current density ~ 100 nA/cm$^2$.

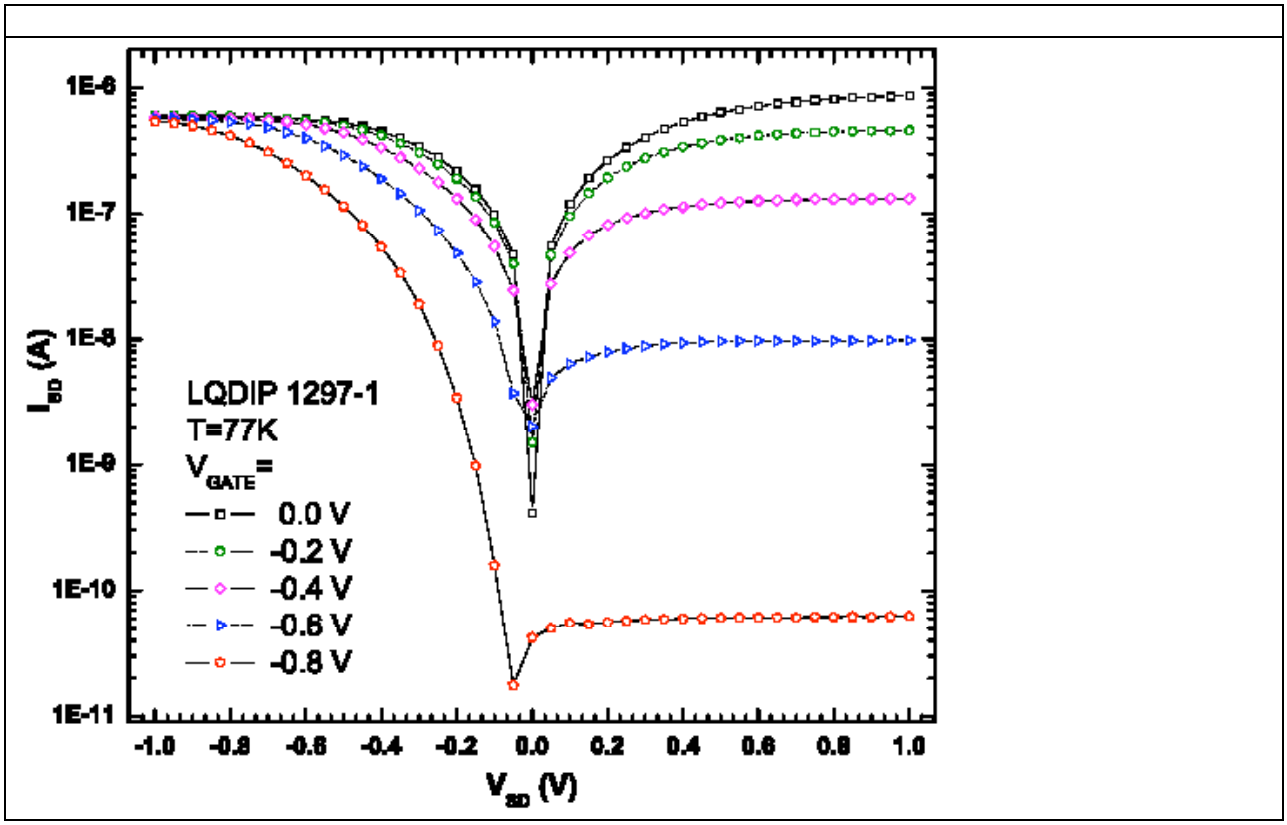


Figure 4: Plot of the source-drain I-V measurements as gate voltage is made more negative.

The strong asymmetry of the $I_{SD}$-$V_{SD}$ results in Fig. 4, illustrated by the relatively small change in $I_{SD}$ as $V_{Gate}$ was made more negative for $V_{SD} < 0$ V, suggests the following. With the asymmetric gate geometry of the LQDIP, the pinch-off gate is located close to the drain contact as shown in Fig. 1, and a wiring configuration where $V_{SD}$ is applied to the drain contact while the source contact remains grounded, as $V_{SD}$ is made negative the size of the depletion-field induced

barrier from $V_{Gate}$ becomes diminished. In contrast, as $V_{SD}$ is made positive the induced barrier from $V_{Gate}$ grows in relative size, leading to a strong depletion effect.

A series of measurements of $I_{SD}$ as a function of $V_{Gate}$ were also taken at different $V_{SD}$. Figure 5 plots the results of these measurements along with corresponding points from the traces in Fig. 4. These plots again show that the gate voltage affects the dark current of the quantum wells differently depending on the polarity of the source-drain bias. When the gate voltage and source-drain bias are of opposite polarity, the gate-field-induced barrier is enhanced as the gate voltage is made more negative leading to a significant decrease in the dark current. For negative source-drain bias, the gate-field-induced barrier becomes diminished and only a small effect on the dark current is visible. The small difference between these traces and the points from Fig. 4 may be attributable to the process of ramping $V_{Gate}$; this is not expected to affect normal device operation where $V_{Gate}$ would always remain constant. Beyond $V_{Gate}$ = - 0.8 V (not shown) the $I_{SD}$ continues decreasing in a roughly similar fashion below the measurement capability of the instrument (~ 1 pA). Finally, the $V_{SD} > 0$ V trace in Fig. 5 shows a monotonic decrease in $I_{SD}$, as $V_{Gate}$ becomes more negative, that casually does not suggest the current in each individual layer of the LQDIP was being cutoff one layer at a time. Whether this behavior is really occurring, however, cannot necessarily be ascertained directly from just an I-V trace, especially at an operating temperature of 77 K which is well above where transport studies of double quantum wells are typically performed (see for example Ref. 13). To more closely investigate the transport behavior differential conductance measurements were performed.

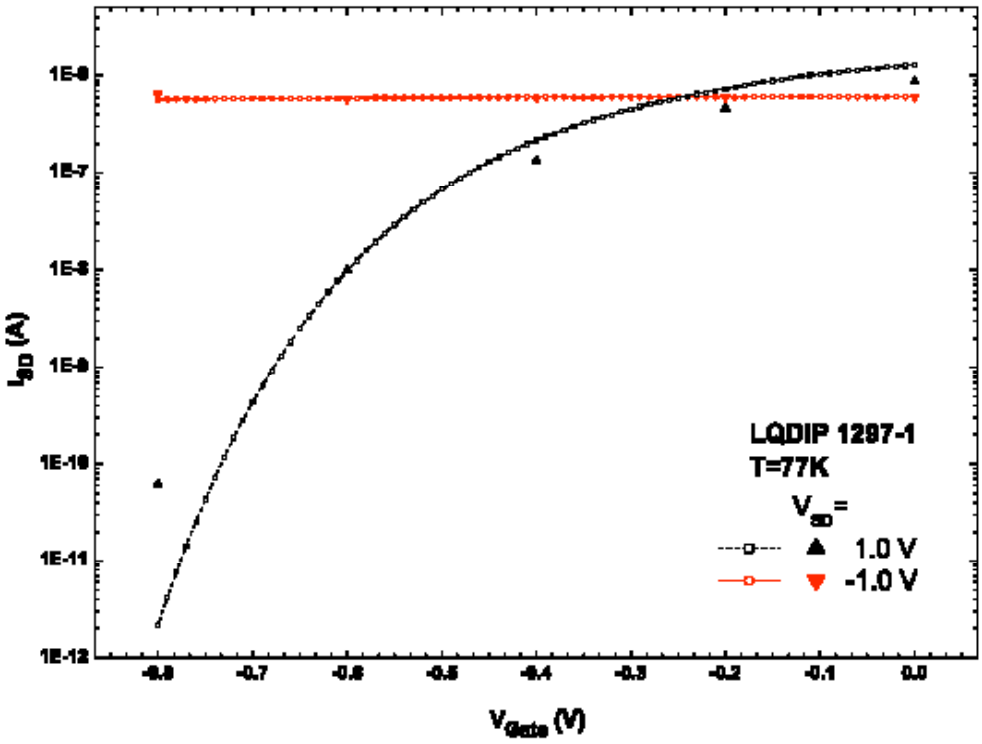


Figure 5: Plot of the source drain current versus gate voltage as various source-drain voltages $V_{SD}$

### 3.2 Differential Conductance Characterization Results

The data for the differential conductance of the LQDIP was gathered by varying the gate voltage and measuring the voltage across a 10 MΩ "sense" resistor, as discussed in Section 2.2. The differential conductance was determined from the measured lock-in voltage, the sense resistance, and the applied 100 μV AC voltage. The conductance at $V_{SD}$ = 0 V is plotted versus the gate voltage, which was varied from 0.0 to -0.85 V in Fig. 6. From Fig. 6 only one large conductance step is clearly visible, appearing to indicate that only one well, the DWELL layer, is being depleted by the negative gate voltage. Closer inspection of this plot, however, reveals the presence of 8 sets of small oscillations in the conductance between $V_{Gate}$ = 0.0 and -0.4 V. These oscillations are most likely due to the presence of quantum dots in the DWELL layer as their presence is not visible in the steps of Ref. 13 and the $\Delta V_{Gate}$ between the steps is ~0.04 V, which, for a lever arm of ~1 for this device structure, would amount to a roughly similar difference (Δ E

~0.04 eV) between the quantum dot energy levels.[14] Thus, this conductance plot suggests that for proper operation of the LQDIP the $V_{Gate}$ should be at least less than ~ -0.4 V, as that will roughly deplete all the quantum dot levels and cut off only the DWELL layer conductance. How much more negative the $V_{Gate}$ should be will require more testing as discussed next.

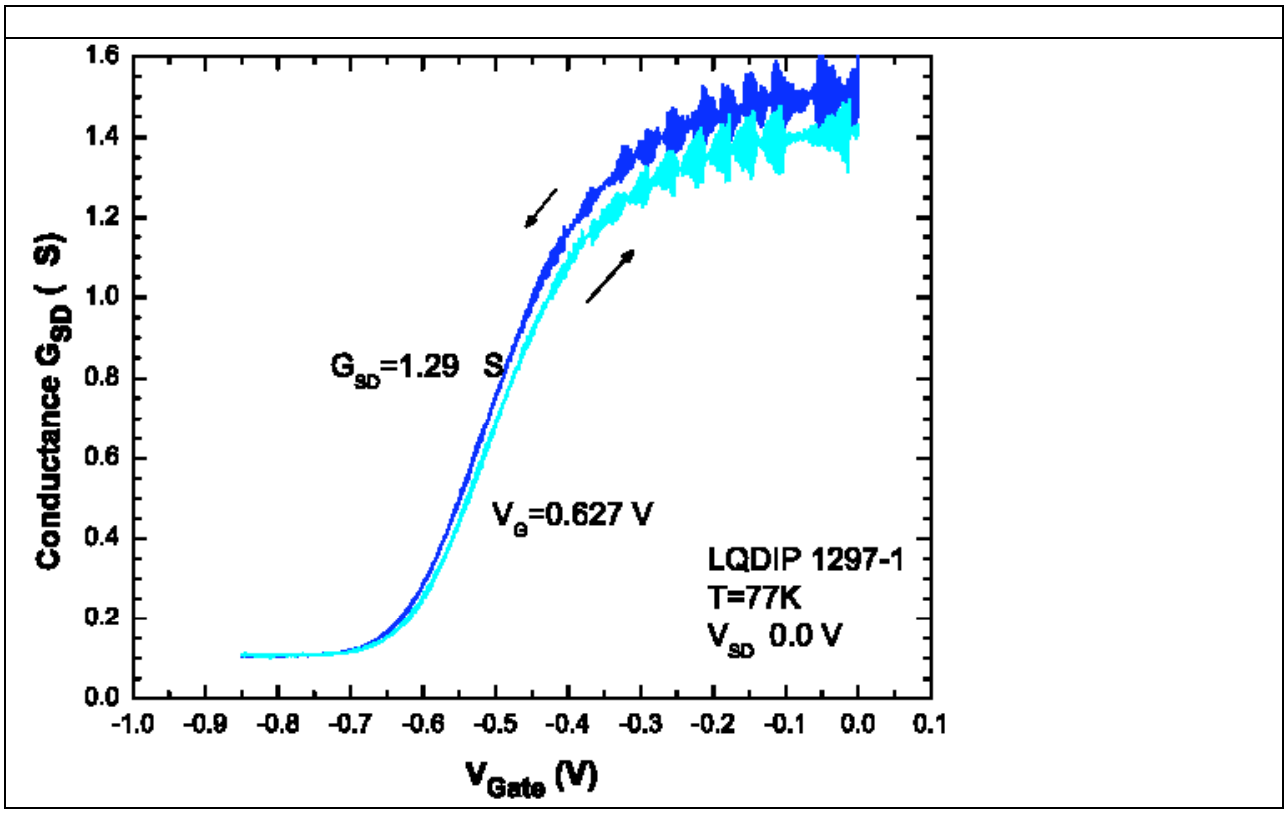


Figure 6: Plots of the differential conductance measurements versus gate voltage.

For conductance measurements on a sample with two equally doped, symmetric quantum wells one would typically expect to see two equally sized steps or drops in the conductance G, one due to each well, as the pinchoff gate voltage was made more negative.[13] The LQDIP, however, is an asymmetric double quantum well where the bottom tuning well is completely undoped, so its conductance properties with respect to $V_{Gate}$ are expected to be different. As the undoped tuning well's conductance is expected to depend directly on the number of carriers that enter it, either via the tunneling, photo-excitation, or relaxation mechanisms, its initial conductance will be smaller than the DWELL layer's. However, how the tuning well's

conductance will initially change as a function of $V_{Gate}$ is not intuitively known as there is some possibility for the tunneling probability to be enhanced as $V_{Gate}$ is initially made more negative and more carriers become available in the DWELL layer to tunnel into it. Thus, the expected number of conductance steps in the LQDIP that will be visible at 77 K is not entirely clear and again, the main guidance we have from Fig. 6 is that the quantum dots in the DWELL appear to become fully depleted beneath the pinchoff gate at $V_{Gate} \sim -0.4$ V, which should at least block the conductance in that layer

### 3.3 Optical I-V Characterization Results

DC photocurrent I-V measurements were then taken to establish the ability of the LQDIP to detect incident blackbody radiation. Figure 7, shows plots of the source-drain I-V with a gate bias of - 0.5 V, in the presence of 300 K blackbody radiation at ~ f/2 with a KRS5 window, as well as a previous dark current measurement under similar $V_{SD}$. As the gate voltage decreases from zero, it is expected to affect photocurrent and dark current somewhat differently. A plot comparing these behaviors is given in Fig. 8. Here, gate voltage is shown to cause a faster decrease in the dark current when compared to the photocurrent. This is a possible indication that the LQDIP's signal-to-noise ratio (SNR) will increase as the gate voltage is made more negative. However, this may also be an indication that the gate behavior is simply less ideal in the presence of light, which was evidenced by some enhancement of the leakage current, or that the small exposed area between the pinchoff gate region and drain contact was allowing for significant absorption to occur in the DWELL.

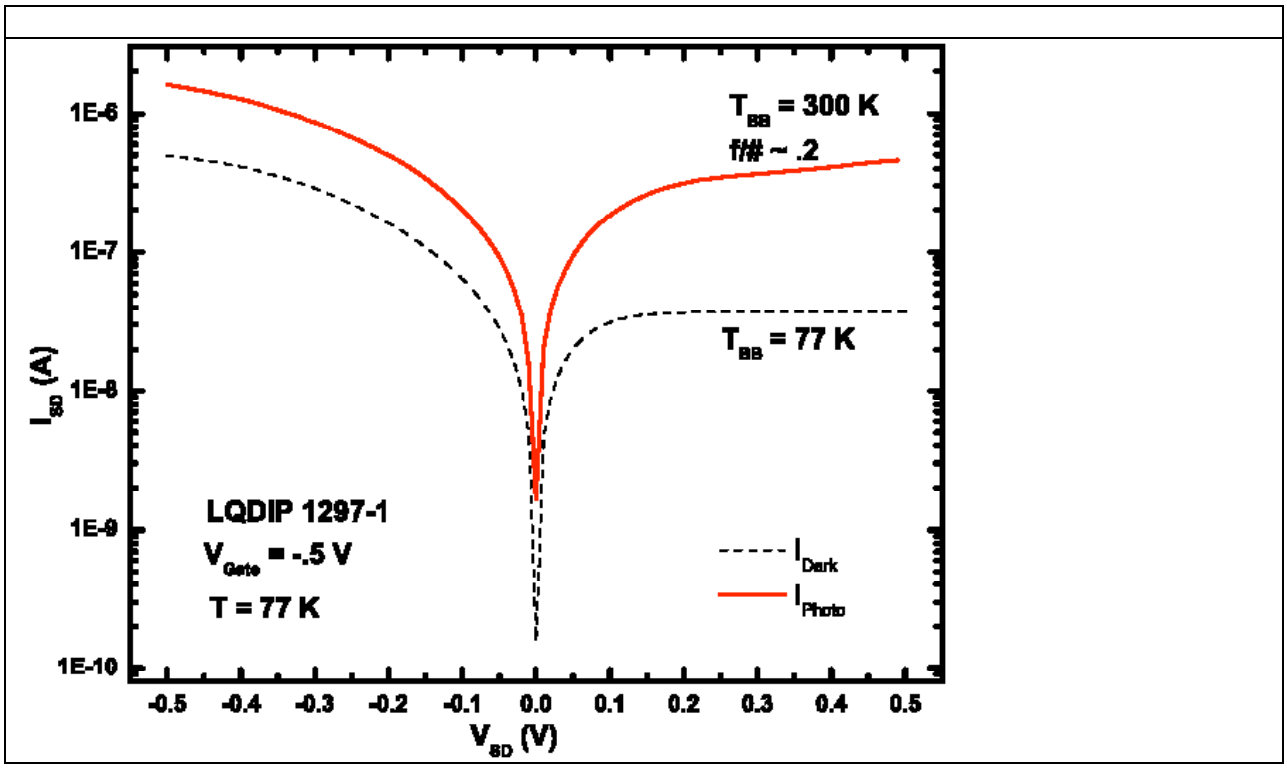


Figure 7: Plots of photocurrent and dark current source- drain I - V measurements

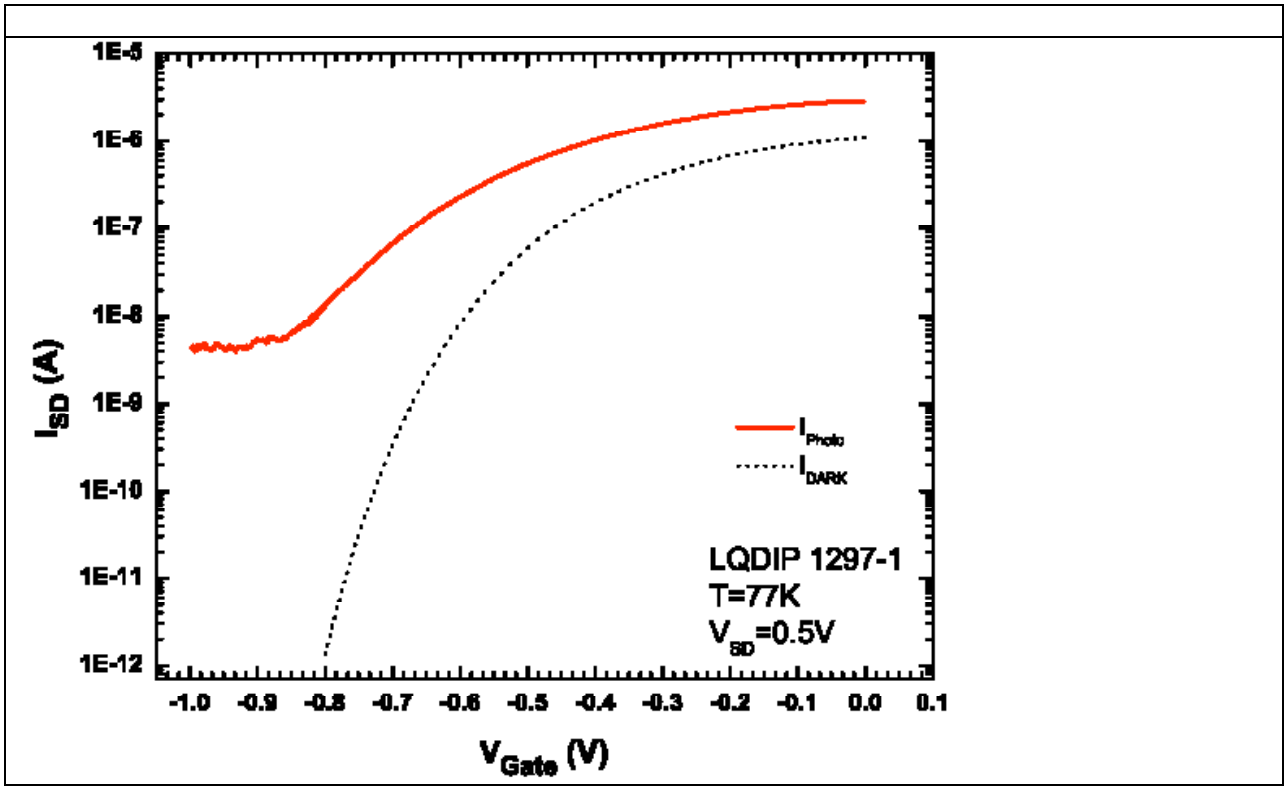


Figure 8: Plots of the source- drain photocurrent and dark current versus gate voltage at a $V_{SD}$ = .5 V.

## 4. CONCLUSION

In conclusion, an LQDIP was fabricated and preliminary I-V and differential conductance measurements were performed. The dark current and photocurrent results showed the expected decrease in dark current and were suggestive of an increase in SNR with an increasingly negative gate voltage. Differential conductance measurement, however, showed only a single step as the gate voltage decreased. This suggests the second quantum well layer may be partially blocked by the gate-induced field as well. Future studies using LQDIPs with multiple gates on both sides of the devices are planned to explore this phenomena.

## 5. ACKNOWLEDGEMENTS

The author would like to acknowledge AFOSR whose funding made this research possible.

## REFERENCES


[1] D. A. Cardimona, D. H. Huang, D. T. Le, T. Apostolova, P. M. Alsing, W. Glass and C. D. Castillo, Proc. SPIE 5897, 58970H (2005)

[2] A. V. Barve, S. Y. Shah, J. Shao, T. E. Vandervelde, R. V. Shenoi, W.-Y. Jang, and S. Krishna, Appl. Phys. Lett. 93, 131115 (2008)

[3] Private Correspondences with David Wellems at AFRL

[4] Meimei Z. Tidrow, William A. Beck, William W. Clark III, Herbert K. Pollehn, John W. Little, Nibir K. Dhar, Richard P. Leavitt, Stephen W. Kennerly, Daniel W. Beekman, Arnold C. Goldberg and Walter R. Dyer, Proc. SPIE 3629, 100 (1999)

[5] D. A. Cardimona, D. H. Huang, B. Feller, M. Landau and C. Morath, Proc. SPIE 7945, 79451J (2011)

[6] V. Ryzhii, Semicond. Sci. Technol. 11, 759 (1996).

[7] L. Chu, A. Zrenner, G. Bohm, and G. Abstreiter, Appl. Phys. Lett. 76, 1944 (2000)

[8] J. Phillips, P. Bhattacharya, S. W. Kennerly, D. W. Beekman, and M. Dutta, IEEE J. Quantum Electron., 35, 936 (1999)

[9] D. Pan, E. Towe, and S. Kennerly, Appl. Phys. Lett., 73, 1937 (1998)

[10] S.-W. Lee, K. Hirakawa, and Y. Shimada, Appl. Phys. Lett. 75, 1428 (1999)

[11] A. D. Stiff, S. Krishna, P. Bhattacharya, and S. Kennerly, Appl. Phys. Lett. 79, 421 (2001)

[12] Private Correspondences with Alvaro Fernandez at Universidad Politécnica de Madrid

[13] J. P. Eisenstein, L. N. Pfeiffer, and K. W. West Appl. Phys. Lett. 57, 2324 (1990)

[14] D. Granados and J. M Garcia, Nanotechnology, 16, S282-S284 (2005).

[15] G. Medeiros-Ribeiro, D. Leonard, and P. M. Petroff, Appl. Phys. Lett. 66, 1767 (1995).

DISTRIBUTION LIST

DTIC/OCP
8725 John J. Kingman Rd, Suite 0944
Ft Belvoir, VA 22060-6218 1 cy

AFRL/RVIL
Kirtland AFB, NM 87117-5776 2 cys

Official Record Copy
AFRL/RVSS/David Cardimona 1 cy

(This page intentionally left blank)